Functional Materials Letters
Vol. 15, No. 5 (2022) 2250022 (4 pages)

DOI: 10.1142/S1793604722500229

World Scientific
www.worldscientific.com

Magnetically driven pH-responsive composite hydrogel for controlled drug delivery

Zhiqin Zhang,[*] Ruofei Wang,[*] Miaofa Yuan,[*] Xuanze Huang,[*] Chen Ding,[*]
Huaping Wu,[†] Shunli Wang[*,‡,¶] and Aiping Liu[*,§,¶]

[*]*Key Laboratory of Optical Field Manipulation of Zhejiang Province*
Zhejiang Sci-Tech University, Hangzhou 310018, P. R. China
[†]*Key Laboratory of Special Purpose Equipment and Advanced Processing Technology*
Ministry of Education and Zhejiang Province, College of Mechanical Engineering
Zhejiang University of Technology, Hangzhou 310023, P. R. China
[‡]*wangshunlisl@163.com*
[§]*liuaiping1979@gmail.com*

Received 2 June 2022; Accepted 28 June 2022; Published 6 August 2022

A multi-footed composite hydrogel with double responsiveness was prepared by the combination of sodium alginate (SA), gelatin and ferroferric oxide nanomaterials. Under magnetic field control, the multi-footed composite hydrogel could walk and move to the designated locations and release some drugs under the specific environment (pH 7.4) due to the pH sensitivity of SA. The gelatin addition effectively improved the mechanical properties of composite hydrogel, adjusting the drug release behavior of composite hydrogel by the decreased porous structure. Our results demonstrated that the proposed dual stimulus-responsive composite hydrogel could offer a promising choice for medical fixed-point drug release and disease treatment.

Keywords: Magnetic actuation; pH sensitivity; composite hydrogel; drug delivery.

At present, the common treatment methods for illness include taking medicine and injection. These pills and injection will flow all over the body with blood movement and be absorbed and eliminated by the human body. However, only a small amount of drug will be absorbed by the pathological area of the human body. Therefore, high dosages or repeated administrations to stimulate a therapeutic effect usually cause the burden of human kidney and other organs, even severe side effects and toxicity.[1,2] In the recent years, hydrogel materials have been widely used as popular vectors for drug delivery, especially oral drug delivery, due to their biocompatibility and similarity to biological tissues.[3] The hydrogels with three-dimensional polymer network can shrink and expand through water loss and absorption under external stimulus, such as temperature,[4–6] electric and magnetic fields,[7–10] pH,[11–14] thereby adjusting the release location and release amount during the drug release process. For example, the sodium alginate (SA), one of the natural polymers originated from brown algae,[15] can be used as a drug carrier to carry out the fixed-point burst release of drugs by the rapid dissolution of alginate matrices in the higher pH ranges (pH>7).[16] However, little or no drug release can actually be controlled effectively due to the high permeability of formed calcium alginate matrix. Therefore, some polymers or proteins such as gums, chitosan, ethyl cellulose and gelatin (GEL) have been adopted to mix with SA to regulate the porous structure of hydrogel and the rate of drug release.[17] Hereinto, GEL, a biodegradable protein obtained from degradative collagen,[18] can alleviate the sudden release of drug to some extent and improve the mechanical properties of SA-based hydrogel as drug carrier. However, this composite hydrogel usually cannot be artificially controlled to reach a specific location for drug release. Therefore, how to make the hydrogel reach the release site for drug release by means of external field control is a problem that needs to be addressed.

Hydrogels loaded with magnetic nanoparticles are easy to be regulated by external magnetic field,[19] presenting the advantages of long-distance, flexible, accurate and high-speed control. In this study, we designed a double responsive hybrid hydrogel with multi-footed structure by introducing ferroferric oxide nanoparticles (Fe_3O_4 NPs) into the system of SA and GEL to allow the crawling and the movement of composite hydrogel as soft actuator under the control of external magnetic field (Fig. 1). The magnetic nanoparticles will be arranged along the direction of magnetic field to form a multi-footed structure under the influence of magnetic field.[20] Additionally, the composite hydrogel with improved mechanical properties and slackened release rate of model

[¶]Corresponding authors.

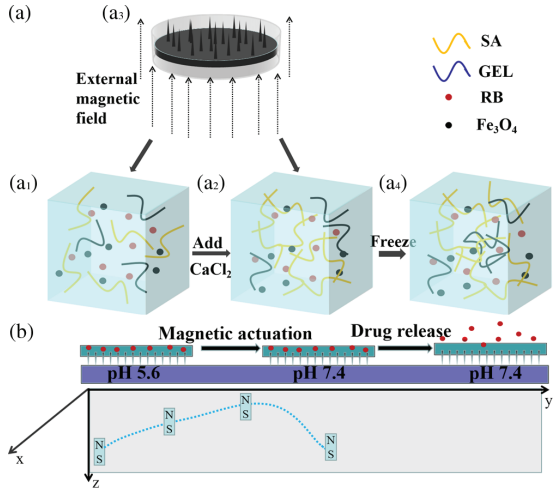

Fig. 1. (a) Preparation of double responsive hybrid hydrogel with multi-footed structure. The precursor including SA, GEL, RB and Fe_3O_4 NPs (a1) was cross-linked with the addition of $CaCl_2$ (a2) and frozen environment (a4) accompanied by the formation of multi-feet under a magnetic field (a3). (b) Movement and drug release of composite hydrogel with double responsiveness.

drug (Rhodamine B, RB) could realize the fixed-point drug release in a specific environment via the pH responsiveness of SA. This design scheme is conducive to the exploration and development of medical soft robot for fixed-point drug release and disease treatment.

The synthesis scheme for double responsive hybrid hydrogel with multi-footed structure is shown in Fig. 1(a). Typically, the precursor solution, including SA, GEL, RB and Fe_3O_4 (20 nm in diameter), was continuously stirred at 37°C for 5 h until completely dissolved without bubbles (the mass ratio of precursor solution to Fe_3O_4 was 3:1, the mass ratio of SA and GEL (SA:GEL) in the precursor solution was set to be 5:0, 5:1, 5:2 and 5:3, respectively). Then, the mixed solution was poured into the petri dish and 0.5 mol/L $CaCl_2$ solution was added and placed for 20 min for the cross-linking of SA molecules. At the same time, a magnetic field of 150 mT was applied to the mixed solution for the formation of multi-feet by the directional arrangement of Fe_3O_4 NPs along the direction of magnetic field. This multi-footed structure could be well preserved after cross-linking of SA molecules when the magnetic field was removed. After that, the sample was put into the freezer for secondary cross-linking to form hydrogen bonds between GEL molecules, obtaining multi-footed composite hydrogel contained RB. Notice that, as a soluble protein with helical structure, the molecular chain of GEL contains a large number of functional groups, such as amino and carboxyl groups, and hydrogen bonds in the molecular chains and between the molecular chains.[19] The hydrogen bonds would disintegrate when the temperature is higher than 40°C, making the spiral structure of GEL unstable and changing to sol state.[21] When the temperature of GEL sol is lower than 40°C, the hydrogen bonds in GEL are re-formed between the chains and the molecules of GEL, leading to the formation of GEL hydrogel.[22] The pure SA, GEL and the composite hydrogel without Fe_3O_4 NPs as controls were also prepared by the similar method.

The morphology and microstructure of hydrogels were observed by a scanning electron microscopy (SEM) under the accelerated voltage of 5 kV. Fourier transform infrared (FITR) spectra of hydrogel samples in KBr were measured on Fourier transform infrared spectrophotometer in the range from 4000 to 450 cm^{-1}. Mechanical properties of hydrogel strips (4 cm × 1 cm × 1.5 cm in length × width × height) were measured in the mechanical testing machine. The movement of composite hydrogel from acidic environment to neutral or alkaline environment was carried out under magnetic driving, and the movement behavior was observed and recorded with a camera when the soft robots were placed on different surfaces with different roughness. The drug load of hydrogels was calculated in the **Supporting information**. The *in vitro* drug release experiment was carried out in the phosphate buffered saline (PBS) at 37°C, and the absorbance of the release solution was obtained on an Ultraviolet visible spectrophotometer (UV-2700).

Figure 2 shows the SEM images of the composite hydrogel. The SA hydrogel presents a homogeneous porous structure (Fig. 2(a)), which is almost covered and filled by GEL after the cross-linking of GEL molecules (Fig. 2(b)). The cross-section SEM images of composite hydrogel also shows smaller pores when compared to that of pure SA hydrogel (Figs. 2(c) and 2(d)). The multi-footed structure is obviously observed from Fig. 2(e) with the length of the micro-foot about 1 cm and the distance between the micro-feet about 0.2 cm (4 cm × 4 cm of the sample).

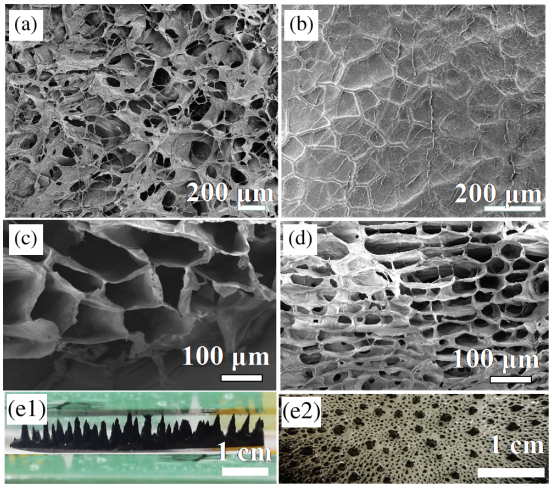

Fig. 2. SEM images of (a) surface of SA hydrogel, (b) surface of composite hydrogel without Fe_3O_4 NPs, (c) cross-section of SA hydrogel, (d) cross-section of composite hydrogel without Fe_3O_4 NPs and (e_1–e_2) multi-footed composite hydrogel with Fe_3O_4 NPs.

Figure 3 shows the infrared spectra, expansion rates and drug (RB) release abilities of different samples. From the FTIR spectrum of pure SA (Fig. 3(a)), the absorption peak at 3430 cm^{-1} is attributed to the free $–NH_2$ group in SA.[23] The peak at about 1630 cm^{-1} is due to the C=O and C–N stretching vibrations in SA.[24] The absorption peaks at 1640 cm^{-1} and 1540 cm^{-1} in the FTIR spectrum of GEL correspond to C=O and C–N tensile vibrations (amide I band) and NH-group bending vibration (amide II band),[25] respectively. Only, peak intensity increase without new peak appearance is verified when RB is wrapped in the composite hydrogel, indicating no interaction between RB and composite hydrogel. The expansion rates of composite hydrogel prepared with different mass ratios of SA and GEL (SA:GEL) are also studied (Fig. 3(b)). It can be seen that the swelling degree of composite hydrogel with SA:GEL=5:1 is about 150%, which increases to about 350% when SA:GEL=5:3. SA has the lowest expansion rate, which is attributed to the unrestrained absorbed water in the SA hydrogel system due to its large pore size (Fig. 2(a)). When GEL is added into the SA system, GEL hydrogel fills the porous structure and the GEL molecular chains in the SA network can absorb and preserve more water, increasing the swelling degree of composite hydrogel. The effect of GEL on the drug release ability of SA is also verified. As shown in Fig. 3(c), the ability to load drugs of composite hydrogel improves with the increasing of GEL in the system. GEL addition not only increases the drug load and cumulative release percent of RB but also adjusts the drug release rate, therefore presenting an effect of sustained release in some degree.

GEL also greatly affects the mechanical properties of the composite hydrogel. Figures 4(a) and 4(b) show the tensile properties of composite hydrogel. When the SA content is fixed, the elastic modulus of composite hydrogel increases from 70 kPa to 181 kPa with the increase of GEL content.

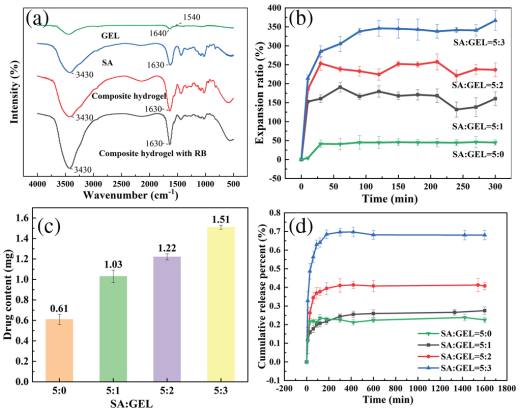

Fig. 3. (a) FTIR spectra of SA, GEL, composite hydrogels without and with RB. (b) Expansion rates of composite hydrogel prepared with different mass ratios of SA and GEL. (c) Drug load and (d) drug release of composite hydrogels with different mass ratios of SA and GEL in pH 7.4 environment.

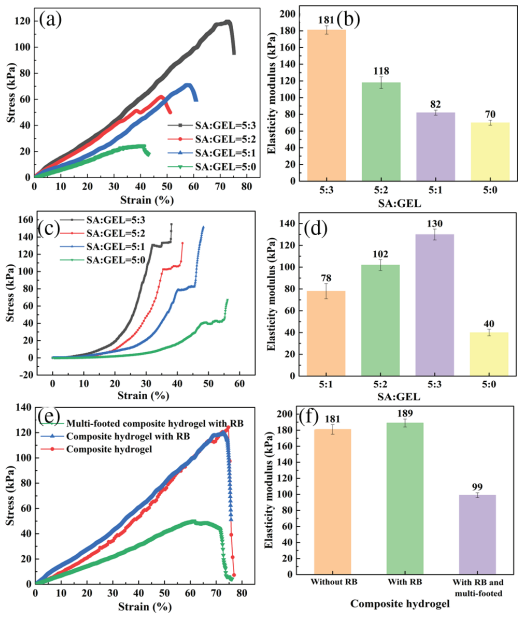

Fig. 4. Mechanical properties of composite hydrogels: (a) Tensile properties of composite hydrogel, (b) elasticity modulus of tension, (c) compression performance of multi-footed composite hydrogel, (d) elasticity modulus of compression, (e) tensile properties of composite hydrogels without and with RB and multi-footed composite and (f) elasticity modulus of tension of different samples.

The compression performance of multi-footed composite hydrogel also presents a similar trend (Figs. 4(c) and 4(d)) with the fracture stress increasing from 40 kPa for pure SA to 130 kPa for composite hydrogel with SA:GEL=5:3. The addition of RB has no obvious effect on the mechanical properties of the composite hydrogel, while the multi-footed structure causes great decrease in the mechanical properties of composite hydrogel, which might be attributed to the decline of hydrogel density after micro-feet formation.

Figures 5(a)–5(d) show the movement ability of composite hydrogel as soft robot under magnetic field control. The soft robot cannot move on the smooth surface when the side without micro-feet contacts with the smooth surface (Fig. 5(a)). By contrast, it can move forward via the micro-feet on this smooth surface due to the reduction of friction between soft robot and solid surface (Fig. 5(b)). The movement of multi-footed composite hydrogel is divided into five steps, as shown in Fig. S1. The movement time spent from end to end increases to 17 s when the solid surface becomes rough (Fig. 5(c)). When the PBS with pH 7.4 is dropped on the soft robot at the moment of 18 s, the colourless PBS turns pink at 94 s, indicating the release of RB drug from composite hydrogel. Therefore, the double responsive composite hydrogel has good magnetic driving performance and can move on both the smooth and rough surfaces under the control of magnetic field to the specific location to release drugs with the pH stimulation. When Fe_3O_4 NPs are added into the composite hydrogel, the release quantity of RB decreases to about 55%

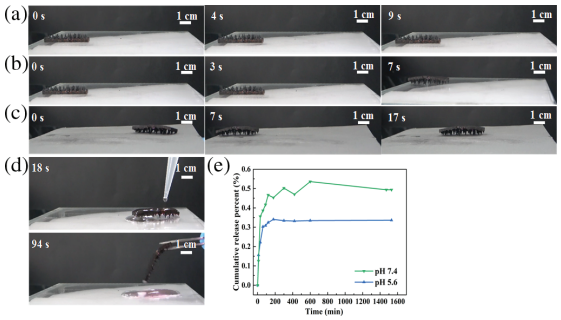

Fig. 5. Optical photographs of the movement process of soft robot on the (a) smooth surface with the side without micro-feet contact with the smooth surface, (b) smooth surface with the micro-feet contact with the smooth surface and (c) rough surface. (d) The dropping of PBS with pH=7.4 on the soft robot and the color change of PBS after RB drug release. (e) Drug release of multi-footed composite hydrogel in PBS with different pH levels.

(Figs. 5(e) and 3(d)) with the release speed slowing down to some degree, which could be attributed to the partial blocking of the pores in the composite hydrogel by Fe_3O_4 NPs. The composite hydrogel presents better drug-release ability at pH 7.4 environment when compared to that at pH 5.6 environment due to the pH-related degradation of SA.[26]

In summary, we have proposed a composite hydrogel including magnetic nanoparticles, which could move via the multi-footed structure under a magnetic field control and release drugs under pH control due to the pH responsiveness of SA. The GEL addition also favors the mechanical properties' improvement and sustained release of drugs due to the reducing hydrogel voids. This strategy can also be applied to the release of different kinds of drugs, therefore has potential application prospects in the field of medical fixed-point drug release and disease treatment in the future.

Acknowledgment

This work was supported by the Zhejiang Outstanding Youth Fund of China (No. LR19E020004), the Youth Top-notch Talent Project of Zhejiang Ten Thousand Plan of China (No. ZJWR0308010) and the Zhejiang Provincial Natural Science Foundation of China (No. LR20A020002).

References

1. J. Li *et al*., *Nat. Rev. Mater.* **12**, 16071 (2016).
2. K. Zhang *et al*., *Chem. Rev*. **121**, 11149 (2021).
3. K. Wang *et al*., *Int. J. Pharm*. **389**, 130 (2010).
4. J. Liu *et al*., *J. Mater. Chem. C* **8**, 12092 (2020).
5. P. L. Dong *et al*., *Adv. Intell. Syst*. **3**, 2640 (2021).
6. C. Yao *et al*., *Adv. Funct. Mater*. **25**, 2980 (2015).
7. Y. Li *et al*., *Adv. Funct. Mater*. **23**, 660 (2012).
8. M. Daniel *et al*., *Soft Matter*. **10**, 1337 (2014).
9. H. W. Huang *et al.*, *Nat. Commun*. **7**, 1 (2016).
10. W. Shi *et al*., *ACS Appl. Mater. Interfaces* **12**, 5177 (2020).
11. M. Kanamala *et al*., *Biomaterials* **85**, 152 (2016).
12. M. Krogsgaard *et al*., *Biomacromolecules* **14**, 297 (2013).
13. H. Bai *et al*., *Chem. Comm*. **46**, 2376 (2010).
14. P. Wei *et al*., *J. Inorg. Organomet. Polym. Mater.* **29**, 659 (2019).
15. A. S. Montaser *et al.*, *Int. J. Biol. Macromol.* **124**, 1016 (2019).
16. A. Ferreira *et al.*, *J. Control. Release.* **97**, 431 (2004).
17. Q. Wang *et al*., *Mat. Sci. Eng. C-Mater*. **99**, 1469 (2019).
18. D. Ribeiro *et al*., *Biomolecules* **10**, 63 (2019).
19. X. Yang *et al.*, *Small* **18**, 2104368 (2022).
20. R. M. Erb *et al*., *Adv. Func. Mater.* **26**, 3859 (2016).
21. S. B. Park *et al*., *Prog. Polym. Sci.* **68**, 77 (2017).
22. Y. H. Qing *et al*., *Adv. Func. Mater.* **28**, 1705069 (2018).
23. X. Zhang *et al*., *Int. J. Biol. Macromol*. **181**, 1039 (2021).
24. S. Sultan *et al.*, *Nanoscale* **10**, 4421 (2017).
25. J. Xing *et al*., *Colloids Surf. B-Biointerfaces* **204**, 111776 (2021).
26. Z. Dong *et al.*, *J. Membr. Sci*. **280**, 37 (2006).